Network: Comput. Neural Syst. **11** (2000) 299–320. Printed in the UK PII: S0954-898X(00)17643-2

Self-organized synchronous oscillations in a network of excitable cells coupled by gap junctions

Timothy J Lewis and John Rinzel

Center for Neural Science and Courant Institute for Mathematical Sciences, New York University, 4 Washington Place Room 809, NY 10003, USA

E-mail: tlewis@cns.nyu.edu

Received 26 April 2000

Abstract. Recent evidence suggests that electrical coupling plays a role in generating oscillatory behaviour in networks of neurons; however, the underlying mechanisms have not been identified. Using a cellular automata model proposed by Traub *et al* (Traub R D, Schmitz D, Jefferys J G and Draguhn A 1999 High-frequency population oscillations are predicted to occur in hippocampal pyramidal neural networks interconnected by axo-axonal gap junctions *Neuroscience* **92** 407–26), we describe a novel mechanism for self-organized oscillations in networks that have strong, sparse random electrical coupling via gap junctions. The network activity is generated by random spontaneous activity that is moulded into regular population oscillations by the propagation of activity through the network. We explain how this activity gives rise to particular dependences of mean oscillation frequency on network connectivity parameters and on the rate of spontaneous activity, and we derive analytical expressions to approximate the mean frequency and variance of the oscillations. In doing so, we provide insight into possible mechanisms for frequency control and modulation in networks of neurons.

(Some figures in this article are in colour only in the electronic version; see www.iop.org)

1. Introduction

The synchronous firing of neurons is evident in networks throughout the cortex and is thought to play a fundamental role in behavioural and cognitive function [17], as well as in regulating development [8]. Often the synchronous activity is rhythmic and can have a wide range of frequencies. The oscillatory behaviour can result from rhythmic correlated input (e.g. due to subcortical oscillations [25]), but oscillations can also arise from the intrinsic dynamics of the cortex [27]. Little is known, however, about the mechanisms that give rise to these oscillations.

Neocortical and hippocampal networks in slice preparations can generate various types of spontaneous network oscillation in the presence of neuromodulators, certain pharmacological agents or modifications in ionic environment. Several studies show that this activity persists in the absence of fast chemical transmission [2,9,23]. Furthermore, the extracellular fields during this activity are small enough to rule out substantial coupling via field effects. These findings, along with recent direct evidence for functional gap junctions in the cortex [13, 14], suggest that electrical coupling via gap junctions could mediate the synchronous network oscillations.

Sometimes network oscillations are clearly generated by the intrinsic oscillatory dynamics of the individual neurons [7,21,22]. In this case, electrical coupling could serve to synchronize activity via phase locking [5]. On the other hand, network oscillations have been observed in many cases in which action potentials arise from baseline without the clear generator potentials

0954-898X/00/040299+22$30.00

that are associated with intrinsic oscillators [2, 9, 23]. Cells in this case are presumably in an 'excitable' state, in which individual cells have stable resting states and fire only when they receive suprathreshold stimuli. It has been suggested that synchronous network activity is generated by random spontaneous events and propagation through the network via gap junctions. Indeed, Traub and coworkers found similar behaviour in detailed models of neurons coupled by gap junctions [26, 28]. The key features of these models were that cells were excitable, each cell had low-frequency spontaneous random activation and electrical coupling was strong and sparse. However, the mechanisms that shape the random spontaneous activity into coherent network oscillations with a particular frequency remained unclear.

In order to elucidate the dynamical mechanisms of the oscillatory behaviour, Traub *et al* [28] proposed a cellular automata (CA) model for networks with strong, sparse electrical connectivity. This model has network connectivity similar to that in the detailed Traub models but has simple rules governing cellular dynamics. The simple model reproduces the network oscillations, indicating that many features of the oscillations are determined purely by the structure of the network and can be described without using detailed biophysical neuron models. Traub *et al* found interesting dependences of the mean oscillation frequency on the rate of spontaneous activity and on network connectivity parameters. However, the mechanisms underlying the oscillations and their dependence on the parameters were not uncovered.

Our goals in this paper are to describe mechanisms giving rise to the oscillatory behaviour in the CA model, to explain the parameter dependences and to discuss their implications for the physiological networks. The relative simplicity of the CA model allows us to accomplish these goals. We show that expanding waves, which arise from the repetitive random spontaneous activity, form the functional units of the oscillatory behaviour. Using arguments based on this observation, we predict statistical features of the oscillations and show how dynamical properties of the network can shape random firing into regular rhythmic activity. These findings could have important implications for how some oscillations arise in the cortex: in neuronal networks that are quiescent in the absence of input, there is no need to have rhythmic input in order to obtain rhythmic network activity. We also show how the frequency of the oscillations can be controlled by modulation of system properties such as network connectivity, rate of random spontaneous events and cellular dynamics.

It should be noted that although the CA model was constructed in order to describe neuronal networks with electrical coupling [28], it could be applicable to any random network of elements with excitable dynamics and strong symmetric (i.e. bidirectional) connections.

2. The CA model: connectivity and rules governing dynamics

The following provides a complete description of the CA model. First, we describe how the connectivity of the network is determined and then give a description of the rules governing cellular dynamics. The model is very similar to the CA model of Traub *et al* [28], but it is slightly more generalized. Connectivity and dynamics in the model are consistent with those in networks with strong and sparse electrical coupling as is the case described in [26, 28].

The model consists of a single-layer network with recurrent bidirectional connections (i.e. activity can be transmitted in both directions). Cells are set on a uniform $n_x \times n_y$ grid. Connections between cells are assigned randomly with the restriction that a cell can only be connected to cells that are no greater than a Euclidean distance r_c cells away from it. In a network with $r_c = 1.5$, a cell has possible connections only to its eight nearest neighbours, whereas a network with r_c greater than the size of the network has all-to-all possible connections and is effectively independent from the grid formulation. Traub *et al* [28] use an intermediate value of $r_c = 10$ in networks of 96×32 cells or larger.

If m connections are inserted into the network, then the average number of junctions per cell in the network is $c = m/M$, where $M = n_x n_y$ is the total number of cells. The value c will be used as a measure of network connectivity. Note that, given a specific connectivity radius r_c, there is a maximal value of c that corresponds to complete connectivity. Obviously this value, which we refer to as c_{max}, increases with r_c. When $r_c = 1$ (four-nearest-neighbour coupling) $c_{max} = 2(n_x - 1)(n_y - 1)/(n_y n_x) \to 2$ as $n_y, n_x \to \infty$, whereas when $r_c > n_y, n_x$ (all-to-all coupling) $c_{max} = (n_y n_x - 1)/2$.

Practically, the network is established as follows. A cell in the network is chosen randomly and then another cell within a distance r_c from the first cell is randomly selected. A connection is made between these two cells. Redundant connections are not allowed and an excess number of connections around the boundaries is avoided by including 'fictitious' cells outside the $n_x \times n_y$ grid during the selection process. The above process is repeated until there are a total of $m = cn_x n_y$ connections between cells in the grid.

If two given cells are within a distance r_c of one another, the probability that they are connected is simply c/c_{max}. Thus, network connectivity can be described explicitly using the probability that two cells are connected:

$$P(d) = \begin{cases} c/c_{max} & \text{for} \quad d \leqslant r_c \\ 0 & \text{for} \quad d > r_c \end{cases}$$

where d is the distance between the cells. $P(d)$ is often called the connectivity footprint [1]. In our case, the connectivity footprint is a circular uniform distribution.

The rules governing the dynamics of the CA are probably the simplest way to describe the dynamical properties of an excitable medium [18,31]. There are three discrete states that a cell can be in: (i) the resting state (also referred to as the recovered state), (ii) the excited state (also referred to as the activated or 'on' state) and (iii) the refractory state. Changes between states can occur during discrete time steps. If a cell is in the resting state and none of the cells that it is connected to are in the excited state, then the cell remains in the resting state at the next time step. On the other hand, if a cell in the resting state is connected to a cell that is excited, then it jumps to the excited state. If a cell is in the excited state, then it changes to the refractory state on the next time step and it remains refractory for $t_r \geqslant 1$ time steps. Following t_r time steps, the cell returns to the resting state, from which it can become excited once more. We set $t_r = 3$ for all simulations presented.

Also, each cell undergoes random spontaneous activation, which is independent from activity in all other cells. This activity is modelled as a Poisson process with rate λ. When a cell is in the resting state and it is selected to become spontaneously activated, it makes a transition to the excited state on the following time step. This random activity provides the basic drive for the network and can be thought to arise from either input from other neural regions or noisy fluctuations intrinsic to the cells.

The changes in activity due to coupling rules and spontaneous activity are updated simultaneously. This is important to point out, because the order of implementing update rules can have a dramatic effect on behaviour in the network as will be explained in the discussion.

Time and distance are dimensionless in the CA. However, for comparison with the pyramidal cell network oscillations in [9, 28], the unit of time, a single time step, can be thought of as the excitation transmission delay between cells, $\sim$0.25 ms, and the unit of space can be thought of as the estimated distance between pyramidal cells, $\sim$20 μm [28]. For comparison with the inhibitory cell network oscillations in [23, 26], our model would have a time step of $\sim$1.0 ms and the unit of space would be $\sim$100 μm.

Before proceeding, we should give a more precise explanation of what is meant by 'sparse' in this paper. A cluster of cells is defined to be a (maximal) set of cells that are interconnected,

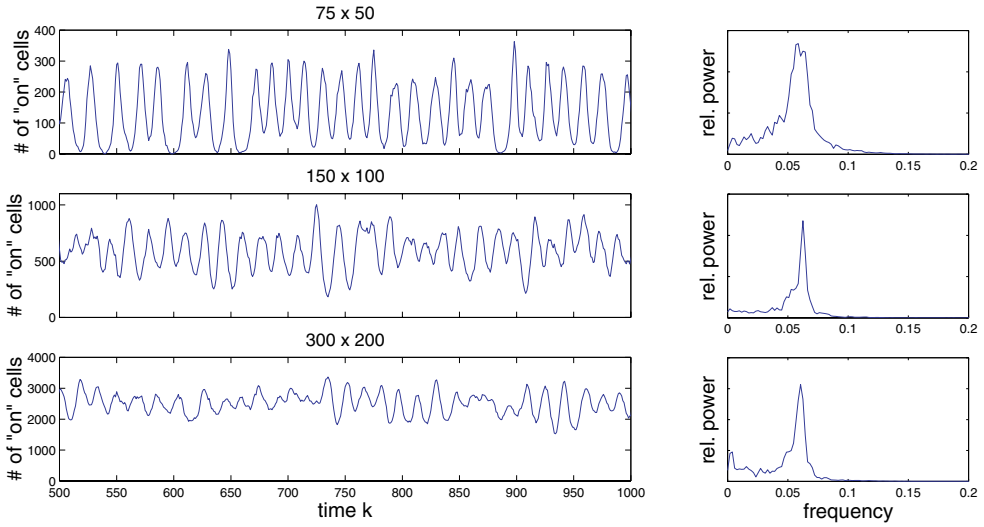

Figure 1. Network oscillations from three networks. The figure shows the number of activated cells as a function of time (left-hand panels) and the corresponding power spectra of the activity (right-hand panels). The networks have different sizes (as labelled), but all other parameters are identical: $\lambda = 0.000\,25$, $r_c = 10$ and $c = 0.8$. To obtain each of the power spectra shown, a 10 000-time-step simulation was divided up into 20 segments of 512 time steps (12-time-step overlaps), and the power spectra of these 20 windows were averaged. There was very little variation between spectra from the individual windows. There was also little difference between the above power spectra and spectra obtained from other simulations using the same parameters.

either directly or indirectly through other cells. For very low c, the network is composed of a large number of small 'clusters', i.e. the size of the clusters is much smaller than the size of the entire network. In this case, there is no mechanism for producing extensive synchronous behaviour. As c increases, a critical value c^* is reached above which there is a large cluster with a size of the same order as the entire network [10, 28]. Note that this critical value of c depends on r_c (and the footprint in general) (unpublished results). The value c^* is known as the percolation threshold [24], because, for c greater than this value, activity can spread or 'percolate' through the bulk of the network. Throughout the paper, when the term sparse is used, the value of c is above the percolation threshold c^* but well below c_{max}.

3. Basic properties of the oscillatory behaviour

Network oscillations can be seen as variations in the number of cells in the excited state (i.e. 'on' cells) with time (k). Figure 1 shows typical examples of the network activity in the CA model with $c = 0.8$ and $r_c = 10$ as in Traub *et al* [28]. When the mean spontaneous firing rate of the individual cells (λ) is 0.000 25, the median frequency of the oscillations is about 0.06, as seen by the peak in the corresponding power spectra in figure 1. Note that this frequency is much larger than λ and is much smaller than the total spontaneous activation rate of the entire network, $M\lambda$ (where M is the total number of cells in the network). It is also much smaller than the inverse of the refractory period. Furthermore, the oscillations are fairly regular. That is, random activation interacts with the intrinsic dynamics of the randomly connected network to produce spontaneously self-organized oscillations.

We observe that these oscillations persist for a wide range of λ, r_c and c (and for a variety of connectivity footprints). Properties of the oscillations, such as mean frequency and variance, vary with changes in parameters. Traub *et al* [28] performed a series of numerical simulations of the CA model with $t_r = 3$ and $r_c = 10$ and showed that the median frequency of network oscillations increases with the rate of spontaneous events λ and with increasing levels of network connectivity c. The above relationships appear to hold for several connectivity footprints (uniform, Gaussian, exponential decay) and the relationships also hold for different footprint widths and refractory period durations (results not shown).

Traub *et al* also suggested that the oscillation frequency is independent of network size. We find that this is effectively true for sufficiently large networks; however, given a small network with fixed λ, r_c and c, the frequency actually increases as the size of the network increases, approaching some maximal frequency. The rate of increase and the maximal frequency depend on λ, r_c and c.

The power spectra in figure 1 show that the peak frequency of the 75×50 network is slightly smaller than that for 150×100 and 300×200. Also, note that the peaks in the power spectra of these larger networks are sharper than for the smaller network. The oscillations in the larger networks appear less regular, and indeed the amplitudes of the oscillations have decreased and are quite variable, but the periods of the oscillations are in fact more regular than that of the smaller network. This tendency for increased variability in amplitude and decreased variability in timing appears to hold for increases in λ, r_c and c independently, but it is not always easy to evaluate the variability in timing.

Mechanisms that determine properties of the oscillations in the CA model should involve both attributes of spontaneous activity and connectivity of the network. It is obvious that the rate of spontaneous activity will affect the oscillatory behaviour and that connectivity determines the ability of a signal to spread through the randomly connected network. However, because spontaneous activity interacts with propagation and refractory properties of the system, it is not clear exactly how the spontaneous firing rate and network connectivity should affect the oscillations. Indeed, it is not even immediately clear how random spontaneous activation of cells in a randomly connected network leads to such regular network oscillations.

Our purpose here is not to provide a complete quantitative description of network phenomena and dependence on network parameters via extensive simulations, but rather to elucidate the dynamical process underlying the behaviour. Insight into this mechanism allows us to see how qualitative features depend on parameters in a natural way. This insight also enables us to derive semi-analytical expressions that show the quantitative dependence of some statistical features of the oscillations, including the frequency, on the system parameters.

4. Propagating waves of activation

In order to uncover mechanisms of network oscillations, it is imperative to understand how activity spreads through the network and how this spread depends on network parameters. In fact, in section 5, it will be shown that the activation profile of a solitary wave of activity can be explicitly used to predict statistics of the network oscillations.

It is easy to see how a propagated wave of activation can form in the CA network. On any given time step, an excited cell will excite resting cells to which it is connected. On the next time step, these newly excited cells will excite resting cells connected to them. As this process proceeds, a wavefront of activation spreads through the network in a cascading fashion. The wave of activation is followed by a wave of recovery to the resting state, the 'waveback'. Because the refractory period is a constant, the wave of recovery follows the path of the wavefront exactly; it is merely delayed by the fixed refractory period, t_r.

In the absence of all other activity and spontaneous input, a wavefront of excitation stemming from a single excited cell spreads through the random network in an organized manner. Because one excited cell can activate several resting neighbours (divergence) and a resting cell can be activated by more than one excited neighbour (convergence), activity will constantly converge and diverge as it percolates through the network. However, all cells that have a shortest pathway of k connections from the original site of excitation will become excited on exactly the kth time step. These cells will return to the rest state at time $k + 1 + t_r$. In this fashion, both the wavefront and the waveback propagate through the network until they reach the boundaries of the cluster on which they reside. As a result of the bidirectional connections, the wavefront propagates as a closed, connected surface in 'network connection space'. This means that there are no paths that lead from cells outside the wave to cells interior to the wave (i.e. in the wake of the wave) without passing through the wave itself. This 'symmetry' of the wave stems from the symmetry of the bidirectional connections and does not exist in random networks with the unidirectional connections associated with chemical synapses. We will show that this property has important implications on how waves interact and therefore on how network oscillations arise.

The waves described above are reminiscent of the waves in target pattern activity seen in partial differential equation models (reaction–diffusion equations) [29] and integro-differential equation models [20] of excitable media. The spread of activity is more complicated in the random networks: instead of propagating smoothly through the medium, the signal percolates through the random network. The waves in both cases, however, form closed connected surfaces in the spatial structures on which they propagate. Thus, despite their geometrical differences, the topologies of the waves are directly analogous to one another. For this reason, we will refer to network behaviour that is entirely composed of these expanding waves as 'topological target pattern activity'. It is important to realize that this topological property of expanding waves is not restricted to random networks with local connectivity. It is a general property of expanding waves in all random networks considered here, even though it is difficult to visualize wavefronts as closed connected surfaces in the complicated network connection spaces associated with $r_c \geqslant 2$.

This section describes the effect that the network parameters (r_c and c) have on wave propagation and the resulting network activity. It also discusses the interaction between waves, as well as the interaction of the waves with spontaneous activity.

4.1. Network connectivity and wave propagation

Let us consider a resting CA network with parameter values $r_c = 10$ and $c = 0.8$. If a cell at the centre of the network is activated at time $k = 1$, then a solitary wave of activity forms and spreads throughout the network as in figure 2. We will take the number of activated or 'on' cells, $N_a(k)$, as a measure of activity in the network. We refer to $N_a(k)$ as the activation profile of a solitary wave.

Despite the fact that the wave of activation forms a closed connected surface on the complicated structure of the random network, the wave appears to propagate as a ring of activity with somewhat diffuse activation. When considering how network parameters affect $N_a(k)$, it is very useful to describe the 'macroscopic' appearance and characteristic features of the wave. It is important however not to confuse these macroscopic properties with the detailed structure of the wave that exists at the level of individual cells and connections.

Figure 2 shows that the fully formed 'macroscopic' wave is well approximated by an expanding annulus with a characteristic width Λ and density of activated cells within the wave α. Although the cell-to-cell propagation velocity of activity is fixed at unity, the macroscopic

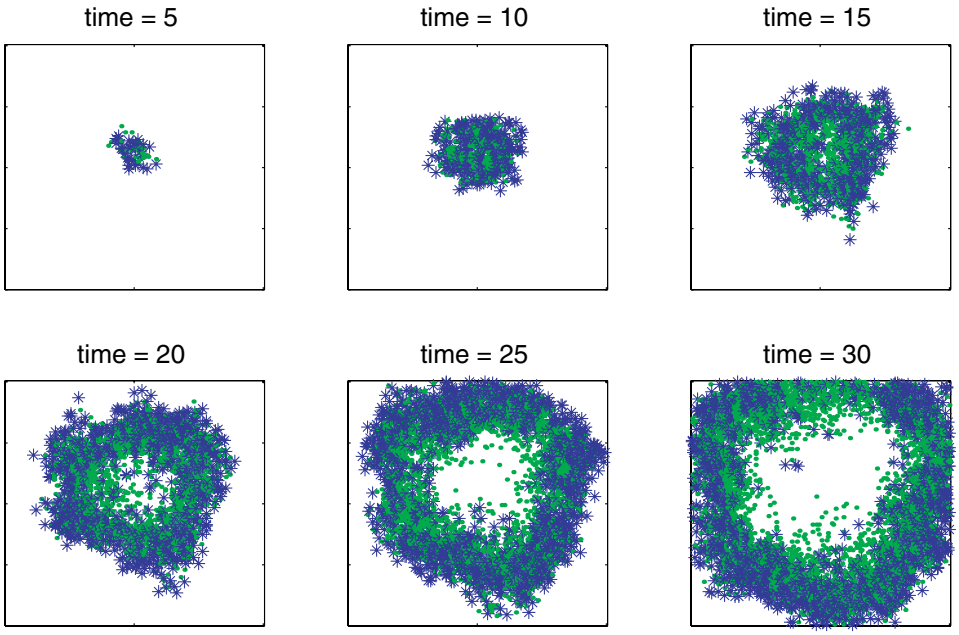

Figure 2. Snapshots in time of a solitary wave of activity in a 200 × 200 network with sparse connectivity ($c = 0.8, r_c = 10$). The wave is initiated at the centre of the network and, following a build-up phase, takes the form of an expanding annulus. Black stars indicate activated cells, grey dots indicate refractory cells and white indicates resting cells.

wave has a constant propagation velocity ν (i.e. there are only very weak curvature effects) and, because the macroscopic wave is composed of activity percolating through the sparsely connected network, ν is substantially less than r_c (approximately five cells per time step in figure 2). The annular shape of the macroscopic wave and the apparently fixed values of Λ, α and ν translate into linear growth in the activation profile, $N_a(k) \sim 2\pi\Lambda\alpha\nu k$. $N_a(k) \sim 70.0k$ in figure 2. This can be seen in figure 3, but it becomes much more obvious when the size of the network is increased.

Prior to the linear growth of $N_a(k)$, there is exponential or superlinear growth in $N_a(k)$ while the full macroscopic wave is being formed. This can be accounted for by activity at the cellular level. During the initial portion of this 'build-up' phase, the probability that two activated cells are connected to the same resting cell is quite low because the number of activated cells is low. Thus, there is a high degree of divergence and infrequent convergence during the spread of activity and $N_a(k)$ grows exponentially. As time progresses, the local density in the forming macroscopic wave increases and the frequency of convergent activity increases. This leads to a progressive decrease in the growth rate of $N_a(k)$ until the macroscopic wave is fully formed, after which $N_a(k)$ grows linearly. After some time, $N_a(k)$ reaches a maximum and then begins to decrease. This is a result of the wave hitting boundaries, filling out the network and dying off.

For different c and r_c, the activation profile of a solitary wave $N_a(k)$ is qualitatively similar to that in figure 3, but there are associated changes in the build-up phase and in Λ, α and ν that lead to changes in the rate of increase in $N_a(k)$. Figure 4 shows that the slope of $N_a(k)$ in the linear growth phase ($N'_a(k)$) increases monotonically with c for $r_c = 10$. Generally, increases

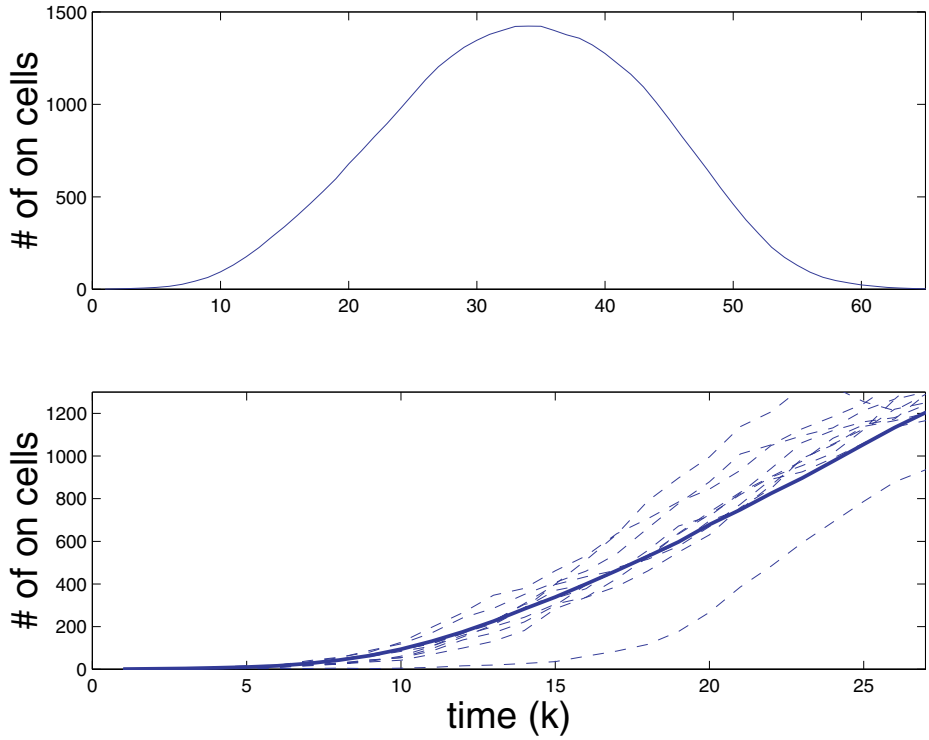

Figure 3. The activity profile for a solitary wave. The number of activated cells $N_a(k)$ during a wave of activity in a 300×200 network with sparse connectivity ($c = 0.8$, $r_c = 10$). Activity is initiated on the largest cluster at a cell in the centre of the network. Solid curves in both the top and bottom panels show the average $N_a(k)$ from 50 networks. The bottom panel is a blow-up of the top panel and includes $N_a(k)$ from ten individual trials (dashed curves). After a period of superlinear growth during the build-up phase of the corresponding wave of activity, $N_a(k)$ grows linearly (more clearly seen in larger networks). When the wave hits the boundary of the network, $N_a(k)$ grows sublinearly and then begins to decreases.

in c or in r_c increase $N_a'(k)$, whereas decreases in c and increases in r_c lead to longer build-up periods. For r_c on the order of the size of the network, although a wave initiated at the centre of the network does expand as a closed connected surface in the network connection space, a geometrical annular wave never forms and therefore there is no linear growth phase in $N_a(k)$. Instead $N_a(k)$ grows exponentially as the wave expands through the network before the growth tapers off and activity dies out due to colliding activity (convergence) and propagated activity reaching deadends in network space.

It is important to point out that $N_a(k)$ is actually a measure of the distribution of path lengths in the random network (i.e. the minimal number of connections between two cells), ignoring the effects of the boundaries. This is simply because propagated activity is incremented by one step in path length during each time step. Therefore, $N_a(k)$ is determined by the network connectivity alone. In section 5, it will be shown that $N_a(k)$ is the key element through which network structure influences the properties of network oscillations, i.e. r_c and c affect network oscillations only through $N_a(k)$.

Unfortunately, $N_a(k)$ can only be explicitly calculated for a few simple cases. In fact, good analytical approximations are difficult to obtain and often are possible only for particular

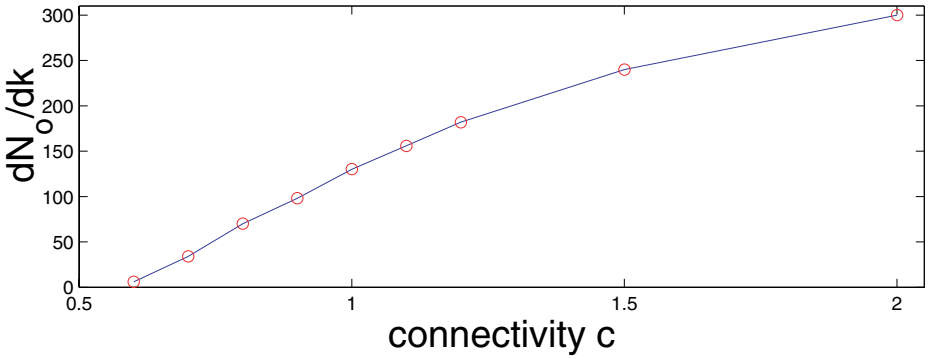

Figure 4. $N'_a(k)$ versus c. Each data point is the approximate slope of the linear growth phase of the average ($n = 50$) activation profile for solitary waves ($N_a(k)$) in 400×400 networks with $r_c = 10$. $N'_a(k)$ is computed by a least-squares fit of $N_a(k)$ from $k = 30$ to 60. (Note that the linear phase for a 400×400 network is substantially longer than that for the 300×200 network used for figure 3.) $N'_a(k)$ should approach $2\pi\alpha\Lambda\nu = 2 \times \pi \times 1 \times 10 \times 10 \simeq 628$ as $c \to c_{max} \sim \pi r_c^2 \simeq 314$.

cases (cf limitations of analytical results from percolation and random graph theory [10, 24]). For now, we leave the activation profile of the solitary wave $N_a(k)$ to be determined empirically and, given that, we show how it can influence network oscillations. We are currently working to obtain quantitative analytical descriptions of how $N_a(k)$ and other network properties depend on connectivity parameters.

4.2. The interaction of waves with spontaneous activity

In the full model, all cells have spontaneous random activity. This leads to multiple sites of wave generation and interactions between the waves generated at the different sites. Thus, the next step towards the goal of understanding network oscillations is to address how waves interact with one another, as well as how spontaneous firing affects activity directly.

If spontaneous activity arises interior to the wave, a new wavefront begins to spread (figure 5, right column). Because the cell-to-cell propagation velocity of the waves is fixed, the new wave propagates away from its site of origin but remains interior to the original wave for all time. If spontaneous activity arises outside an expanding wavefront, a new wave begins to spread from the site of this spontaneous event (figure 5, left column). Because the new wave and the old wave expand as closed connected surfaces, they will eventually collide. Refractoriness behind the wavefronts causes local annihilation of the colliding portions of the waves. The waves then coalesce and form a single larger expanding wavefront of activation, that spreads as a closed connected surface, i.e. the topology of the new wave is the same as that of the individual waves prior to collision. The wakes of the waves also coalesce to form one larger wake. Figure 5 shows these interactions for networks with eight-nearest-neighbour random connectivity, but interactions are topologically equivalent for all r_c and c.

This demonstrates an extremely important characteristic of activity in these networks: it is impossible for activity arising outside an expanding wave to re-activate a cell within the wake of the wave. A cell within the wake of the wave can only be activated by activity spreading from a site within the wake of the wave.

There is another type of wave interaction that can occur in the CA model in general, but it cannot occur in our simulations or in those of Traub *et al* [28]. This type of interaction can

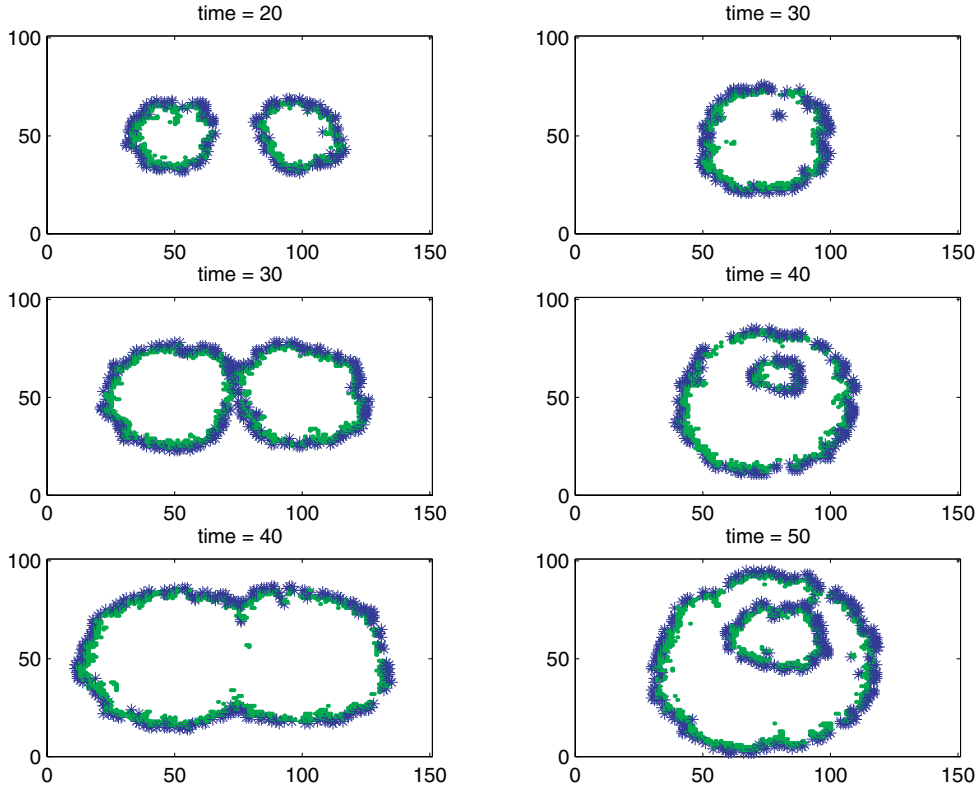

Figure 5. Interactions between propagated waves of activity in a network with sparse connectivity ($c = 1.5$, $r_c = 1.8$). Black stars indicate activated cells; grey dots indicate refractory cells. Left column, waves of activity that arise outside each other's wakes. The waves collide and there is local annihilation of the colliding portion of the waves. The remaining portion of the waves coalesce, forming a single large wave. Right column, activity arising within the wake of a previous wave remains interior to the previous wave. The waves do not affect one another.

occur if a spontaneous event activates a cell immediately behind a waveback. In this case, excitation can spread away from the preceding waveback, but it cannot spread in the direction of the old waveback because the cells in this direction are refractory. Thus, there is 'one-way' block and a wavefront will form that is not a closed connected surface, i.e. symmetry is broken. This broken symmetry can allow the formation of re-entrant behaviour or 're-entry', which is persistent activity circulating around a loop in connection space.

The order of updating the network with respect to spontaneous activity and propagated activity determines whether or not re-entrant activity can occur. Assume that, at time k, a cell in the resting state is randomly selected to be spontaneously activated. One could either set the cell to be active immediately and then update activity by the coupling rules or one could update changes in activity due to propagation and spontaneous activity simultaneously. In the former case it is possible to obtain spontaneous excitation immediately behind a wave and induce re-entry, whereas in the latter case it is impossible to excite a cell immediately behind a wave and re-entry cannot occur. This issue is explained in detail in the discussion (subsection on re-entry) and in figure 9.

5. Network oscillations

We can now turn directly to the goal of identifying and explaining mechanisms that generate the CA network oscillations described in section 3. The spontaneous random activation of cells leads to the formation of multiple expanding waves of activity. These waves interact with one another by colliding and coalescing, but the underlying symmetry is always maintained and all wavefronts are closed connected surfaces in network connection space. This implies that the oscillatory network behaviour seen in figure 1 must be due to topological target pattern activity. That is, network activity is composed solely of expanding waves with centres that are constantly, but fairly locally, shifting in network connection space. Thus, the network divides into ephemeral oscillating units.

Figure 6 depicts macroscopic target pattern activity for a 400×400 network with $r_c = 10$, $c = 1.0$ and $\lambda = 0.000\,05$. What is not apparent in the figure is the underlying topological target pattern structure. The bands of activity seen at the macroscopic level actually form closed connected surfaces in the space defined by the network connections. For smaller networks (e.g. 75×50 or 96×32 as in [28]), the macroscopic structure may be difficult to see or it may not exist at all. The topological target pattern activity, on the other hand, is present in systems of any size and with any set of parameters.

5.1. Limiting behaviour

At very low rates of spontaneous activity, each spontaneous event spreads through the entire network and then the network waits for the next spontaneous event. The effective spontaneous activity rate for the network is λM. In accordance with the underlying process being a discrete Poisson process, the frequency of network oscillations should be approximately $(1 - e^{-\lambda M})$, i.e. assuming that the expected waiting time for a spontaneous event to occur is much larger than the refractory period and the time for the signal to propagate through the network. Note that the important parameter in this case is the effective network spontaneous activation rate λM, the product of the rate with which each cell experiences spontaneous activation λ and the size of the network M.

At extremely high rates of spontaneous activity, the frequency is set entirely by the refractory period t_r; the frequency should be approximately $1/(t_r+2)$ (period of oscillations are the refractory time plus the excitation time). That is, all cells fire as fast as possible, resulting in a maximal frequency. This behaviour is independent of the size of the network.

Network activity is not usually well approximated by these limiting cases. When spontaneous firing rates are in the intermediate range, interactions between waves of activity and spontaneous events lead to behaviour that is more complex and interesting than the limiting cases.

5.2. Wave propagation and mean frequency of network oscillations

By linking the network oscillations to the underlying topological target pattern structure, one can begin to understand how the frequency of the oscillations is set and how its dependence on parameters arises. During repeated random activity, a wave will start at a particular site and propagate outward. Behind this wave, cells wait to be excited again by a new wave. This new wave must start somewhere within the wake of the first wave, because exterior waves of activation cannot penetrate the refractory zone of the first wave. Exterior waves will simply collide with the first wave and lead to the coalescence of the waves and their wakes. Therefore, the mean number of recovered cells that are available to spontaneously fire behind waves of

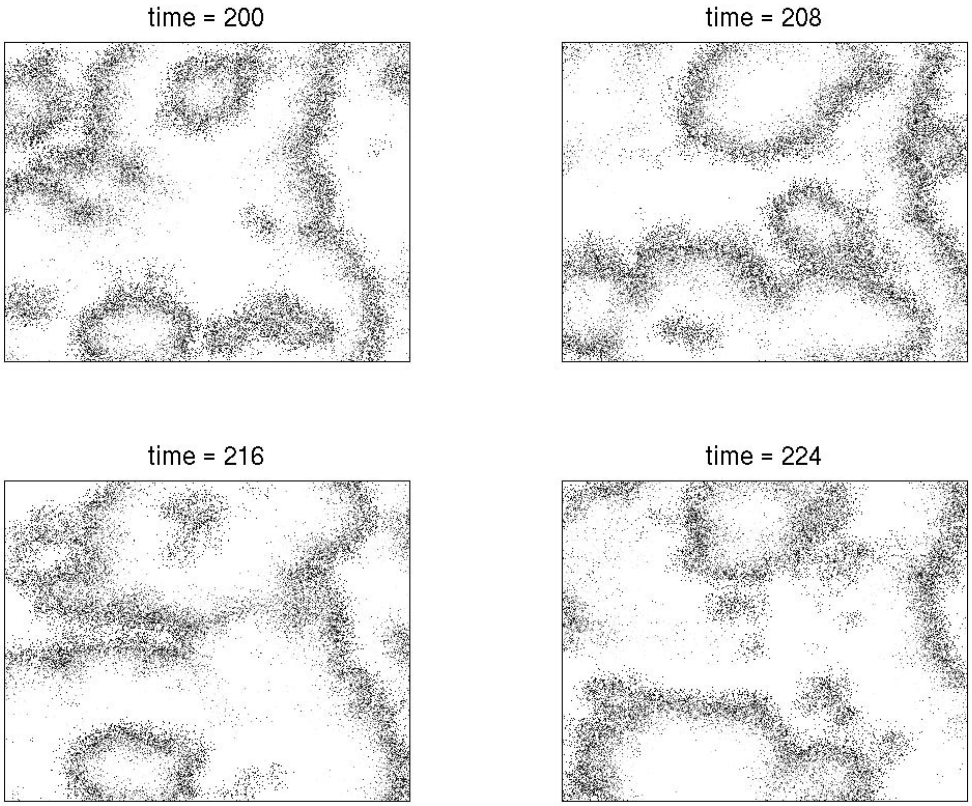

Figure 6. Snapshots in time of network oscillations in a 400 × 400 network with $r_c = 10.0$, $c = 1.0$ and $\lambda = 0.000\,05$. A black point indicates that a cell is activated or 'on'; grey points indicate that cells are refractory; white indicates resting cells. Activity is composed of topological target patterns with constantly shifting centres.

activation and the rate at which cells spontaneously activate (λ) should set the time between successive wave initiations and, in turn, the mean frequency of the network oscillations.

Suppose that we know the mean number of recovered cells that are in the wake of an activation wave at time k, $N(k)$. By taking into account the nature of network activity, we can derive an expression for the probability distribution of waiting times before spontaneous activity occurs within the recovery wake of a wave and starts a new wave. From this probability distribution, we can calculate the expected waiting time to the formation of a new wave and therefore the mean frequency of the network oscillations.

Recall that each cell independent of the other cells is selected to spontaneously fire based on a Poisson process with rate λ. Therefore, for any given cell, the probability for the waiting times to spontaneous firing to be greater than time t is

$$p(t;\lambda) = \mathrm{e}^{-\lambda t}$$

and the probability that a given cell does not fire in each time step is

$$p(1;\lambda) = \mathrm{e}^{-\lambda}.$$

The number of available cells behind a wave is $N(k-1)$ at time $k-1$. The probability that all $N(k-1)$ cells do not fire during the next time step is the product of the probabilities that

each cell does not fire

$$p_{N(k-1)}(1;\lambda) = \prod_{i=1}^{N(k-1)} p(1;\lambda) = \mathrm{e}^{-\lambda N(k-1)}.$$

The probability that all cells have not fired after time $k-1$ is

$$P(k-1;\lambda) = \prod_{j=1}^{k-1} p_{N(j)}(1;\lambda) = \mathrm{e}^{-\lambda \sum_{j=1}^{k-1} N(j)}.$$

The probability that the first firing occurs at time k is the probability that all cells have not fired after $k-1$ steps multiplied by the probability that any cell fires on the kth time step (i.e. one minus the probability that no cells fire on that step):

$$P^*(k;\lambda) = [\mathrm{e}^{-\lambda \sum_{j=1}^{k-1} N(j)}][1 - \mathrm{e}^{-\lambda N(k)}].$$

If $k = 1$ is the time at which the first cell recovers behind an expanding wave, then the expected waiting time for activation of any cell within the wake of the wave is

$$\langle T \rangle = \sum_{k=1}^{\infty} k P^*(k;\lambda) = \sum_{k=1}^{\infty} k \mathrm{e}^{-\lambda \sum_{j=1}^{k-1} N(j)}(1 - \mathrm{e}^{-\lambda N(k)}),$$

which simplifies to

$$\langle T \rangle = \sum_{k=1}^{\infty} \mathrm{e}^{-\lambda \sum_{j=1}^{k-1} N(j)}.$$

Because $N(j)$, the number of recovered cells in the wake of a wave, is a nondecreasing function in j, this sum of exponentials converges for all $\lambda > 0$. Thus, the frequency of network oscillation is expected to be

$$\langle f \rangle = 1/(t_\mathrm{r} + 1 + \langle T \rangle).$$

The variance in the period of oscillation can also be computed:

$$\sigma^2 = \sum_{k=1}^{\infty} (k - \langle T \rangle)^2 P^*(k;\lambda).$$

5.3. Estimate of $N(k)$ using a solitary wave

Many of the qualitative aspects of the network oscillations, as will be described in the following section, can be obtained using qualitative descriptions of $N(k)$ (e.g. $N(k)$ is a nondecreasing function with an asymptotic maximal value; the rate of increase of $N(k)$ is greater for larger c and r_c), but we also would like to obtain quantitative estimates of frequency and variance of the oscillations. In order to do this, we need an approximation of $N(k)$. The effects of the collisions and coalescence of waves on $N(k)$ are quite variable and difficult to characterize. For this reason and because expanding waves form the basic units of the network oscillations, we approximate $N(k)$ using the average number of recovered cells behind a solitary expanding wave.

As mentioned previously, the wave of recovery follows the wave of excitation exactly and is merely delayed by the refractory period t_r. Therefore, the number of recovered cells behind a solitary wave at time k is

$$N(k) = \sum_{j=t_\mathrm{r}+1}^{k+(t_\mathrm{r}+1)} N_\mathrm{a}(j - (t_\mathrm{r} + 1)).$$

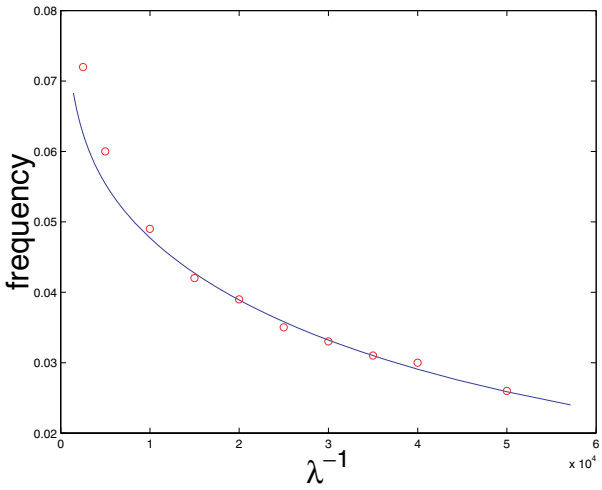

Figure 7. Frequency of network oscillations as a function of the inverse of the spontaneous rate. Circles represent median frequencies obtained from simulations of the full CA model with $t_r = 3$, $c = 0.8$, $r_c = 10$ and a 75×50 network. The solid line shows the predicted frequency, which is calculated using the expression derived in the text. The $N_a(k)$ that was used for the calculation was generated empirically by averaging the activation profiles of solitary waves in 50 networks (with parameters as above).

$N_a(j)$ is the number of cells activated at time j during propagation of a single wave, i.e. it is exactly the activation profile of a solitary wave as described in the previous section. We are currently restricted to computing approximations of $N_a(k)$ empirically. We obtain these approximations $N_a(k)$ for fixed values of c and r_c by averaging the activation profiles of solitary waves initiated in the centre of 50 realized networks. Using this approximation technique, the expression for the expected frequency actually yields excellent estimates over most of the range of λ considered by Traub *et al* [28] (figure 7). On the other hand, in general, the interaction of waves can cause problems for the estimation of the frequency. When the coalescence of the wakes of two colliding waves occurs prior to new activity arising in the wakes of waves, there will be errors in our approximation of the average number of cells in the wake of a wave. This leads to inaccuracies in the frequency estimation. We will address this concern further in the following section.

5.4. Properties of the network oscillation

Although there is no simple scaling of $\langle f \rangle$ with λ, $\langle f \rangle$ is a strictly increasing function of λ with

$$\lim_{\lambda \to \infty} \langle f \rangle = 1/(t_r + 1), \qquad \lim_{\lambda \to 0} \langle f \rangle = 0.$$

This agrees with the behaviour found in simulations. In fact, figure 7 shows the values obtained from the expression for mean frequency and the approximation of $N(k)$ are in excellent quantitative agreement with results from simulations. The simulation data are for 75×50 networks with $c = 0.81$ and $r_c = 10$ (the approximation of $N(k)$ was obtained using these parameters as well). The parameter values, the range of λ and the corresponding data are similar to those in figure 16A of Traub *et al* [28].

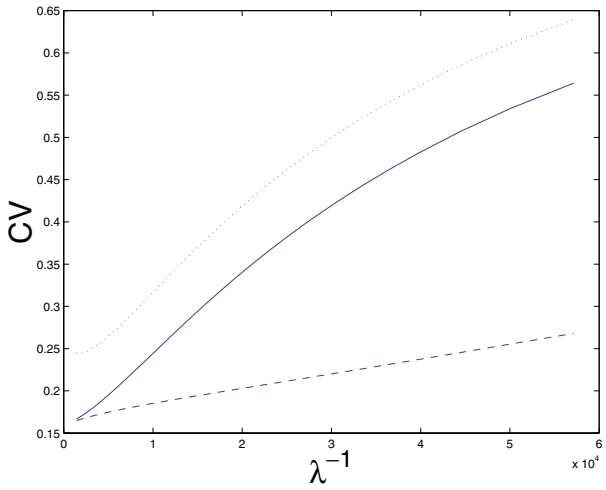

Figure 8. Estimates of the coefficient of variation CV for the period of network oscillations as a function of the inverse of the spontaneous rate ($t_r = 3$, $c = 0.8$ and $r_c = 10$). The solid curve is for a 75×50 network and the dashed curve is for a 150×100 network. The dotted curve is the CV calculated without the effect of the refractory period for the 75×50 network ($t_r = 0$). CV was calculated using the expression derived in the text. The $N_a(k)$ functions used to generate the CV curves for the 75×50 network and the 150×100 network were the average activation profiles of solitary waves in 50 realizations of the 75×50 network and the 150×100 network, respectively.

The dependence of $\langle f \rangle$ on c is implicit in its dependence on the number of cells recovered behind the wake of the wave $N(k)$ (see section 4.1). The larger c is, the faster $N(k)$ increases with k and the faster the exponential terms in the series for $\langle T \rangle$ decay with k. Thus, increases in c lead to shorter waiting times $\langle T \rangle$ and higher frequencies of the network oscillations. A similar relationship holds for r_c and $\langle f \rangle$.

There is also a similar explanation for why $\langle f \rangle$ also depends on the size of the network. In section 3, we state that for small networks frequency increases with the size of the network, and in large networks frequency appears to be independent of size. Note that, when the size of the network is increased, the value of the sums in the exponents for large k increases, causing a decrease in the waiting times between spontaneous events and an increased frequency of oscillation. Put into physical terms, at large waiting times, all waves of activity have propagated to the boundaries of the network and died out. As network size increases, there will be more cells in the wake of a wave that can spontaneously fire. This increases the probability that a spontaneous event will occur at these large waiting times and decreases the expected time until the next spontaneous activation. This mechanism for decreased period, and thus increased frequency, has a small effect whenever the expected waiting time is much shorter than the time that it takes a signal to propagate throughout the network, but it can have substantial effects otherwise.

The predicted coefficient of variation for the period of the oscillations is

$$\mathrm{CV} = \sigma/(t_r + 1 + \langle T \rangle)$$

and is a good measure of the regularity of the oscillations (in terms of period, not amplitude). The solid curve in figure 8 shows the relationship between the predicted CV and λ for a 75×50 network with $c = 0.81$ and $r_c = 10$. The $N_a(k)$ used for the predicted frequency in figure 7 was used to compute the CV. We see that CV is much lower than one, which would correspond to a simple Poisson process. As expected, CV goes to one as $\lambda^{-1} \to \infty$, and CV goes to zero

as $\lambda^{-1} \to 0$. In figure 8, CV is shown to decrease monotonically as λ^{-1} decreases, but it may be interesting to note that at low values of λ^{-1} (below those shown in figure 8) there is a brief range over which CV can increase as λ^{-1} decreases.

When the average activation profile of a solitary wave $N_a(k)$ is empirically generated using larger network sizes, CV decreases as the size of the network increases (e.g. the dashed curve in figure 8 is for a network of 150×100). Similarly, CV also appears to decrease for increases in c and r_c. These observations are consistent with qualitative observations from simulations of the full CA model, where the predominant peak in the power spectra of network activity sharpened as λ, c, r_c and size of network increased.

Note that the above expressions for $\langle T \rangle$, $\langle f \rangle$ and CV are perfectly general and the above results show that the predicted mean frequency of oscillation can be quite accurate. The estimates, however, are only as good as the measurements or approximations of $N_a(k)$ allow them to be. We use functions $N_a(k)$ obtained from averaging the activation profiles of solitary waves started in the centre of 50 realizations of the networks. Thus, in repetitive activity, deviations of the properties of network oscillations from the predictions could be due to several things.

One complicating factor is the effect of boundaries. When a wave is initiated near a boundary, the corresponding wave of recovery could hit the boundary before the next spontaneous activation occurs. The effect of this is to alter the growth of $N_a(k)$, which will lead to an underestimate of the expected waiting time and an overestimate of the frequency of oscillation. These direct boundary effects will be minimal when the network is large.

Another effect that reduces the accuracy of the predicted frequency comes from the interactions between waves. By using the average number of recovered cells in the wake of a solitary wave for $N(k)$, we assumed that frequency is independent from activity exterior to the corresponding excitation wavefront. This ignores the fact that exterior waves can have indirect effects on expected waiting time to next activation. When a wave coalesces with another wave to form a single wave, the regions behind the waves also coalesce (see for example figure 5, left column). This leads to an immediate jump in the number of cells behind the waves whose activation can lead to activation of other cells in that region. The prediction of the mean waiting time does not take this into account, and therefore there is an underestimation of frequency.

We are currently working to obtain quantitative results concerning the effects of wave interactions (i.e. collision/coalescence) on the accuracy of our estimation of frequency, but there appears to be a complicated (nonmonotonic) interdependence on the rate of spontaneous activity λ, and the path length distribution, which is set by network connectivity parameters r_c and c.

Changes in parameters that increase the frequency of collisions appear to generally cause greater underestimation of the frequency. Figure 7 shows that the effects of wave interactions are small over most of the range of λ^{-1} studied, but the effects become apparent at the higher frequencies due to increased wave interactions. The size of the network also affects the accuracy of the frequency estimation, because increased size of the network results in more wave collisions.

It is important to note however that only collisions prior to spontaneous activity occurring in the wake have an effect on frequency; collisions and coalescence after new activity arises have little or no effect on frequency. There are two implications of this. The first is that although it is true that collisions of waves in a large network are abundant, most of these collisions have a very limited effect on frequency. The second implication is that despite the fact that an increase in λ increases the frequency of collisions, it also decreases the waiting times for spontaneous activity to occur in the wake of a wave, which acts to decrease the number of collisions that effect accuracy. These antagonistic processes could lead to nonmonotonic relationships between accuracy and λ.

A similar relationship could exist between accuracy and its dependences on r_c and c. Increases in r_c or c decrease the effective distance (path lengths) between cells, which decreases the time before collisions of waves initiated at two different sites. On the other hand, increases in r_c or c also decrease waiting times for spontaneous activity to occur in the wake of a wave; this acts to decrease the number of collisions. Thus, it is not immediately apparent how changes in r_c or c should affect accuracy of the predicted mean frequency.

It is easy to explain the qualitative dependence of regularity of amplitude of the oscillations on the network size in the context of the described mechanism. We pointed out that, as the size of a large network grows, the regularity of amplitude in the oscillations decreases (see figure 1). This is simply due to the fact that large networks support multiple waves and, in general, these waves will be out of phase with one another (i.e. expanded to varying radii). The larger the network is, the more waves with different phases it supports. This in turn causes the oscillations to have a decreased maximal peak-to-peak amplitude and to appear more irregular in amplitude.

6. Discussion

In this paper, we describe a self-organizing mechanism by which regular oscillations can arise in a network of cells that is randomly coupled by gap junctions and forced by random spontaneous activity (or input). Network activity is composed of expanding waves stemming from the spontaneous activity. Because connections are bidirectional and dynamics include a refractory period, these waves form closed connected surfaces that are impenetrable to activity outside the wave. Thus, reactivation of cells within the wake of a wave must derive from spontaneous activity arising within the wake, and the frequency of the network oscillations is set by the mean waiting time for new spontaneous activity to occur within the wake. By identifying the mechanism of the oscillation, we are able to qualitatively explain the dependence that frequency has on system parameters. In some parameter regimes, we can also quantitatively predict the mean frequency of the oscillations. The mechanism also points to how a relatively small CV in the period of oscillation can arise despite the random nature of both the network and the Poisson input.

The CA model

Cellular automata have been used to successfully model many systems [11]. For example, the CA model used in this paper, but restricted to complete nearest-neighbour connectivity, has been used to study electrical activity in heart tissue and has provided important insight into the dynamical underpinnings of cardiac arrhythmias [18, 19, 31]. Also, Butts, Feller and colleagues [4, 12] have recently elucidated mechanisms underlying irregular spatiotemporal patterns of activity in the developing retina using a CA model.

CA models have several shortcomings. Time and states are discrete variables, and dynamics are governed by very simple update rules. In the CA model considered here, cells consist of only single compartments. There is also a lack of detailed ionic membrane dynamics and realistic gap junction conductances. However, the strengths of CA models stem from these same aspects. The models are designed with the intention of capturing the essential dynamical principles of the system. The resulting simplicity often allows the dynamical mechanisms underlying the behaviour of the system to become strikingly evident. Indeed, by studying a CA model, we are able to identify a potential mechanism for network oscillations and show how features of the oscillations can depend purely on the network structure.

All results obtained here are for the CA model, but the generality of the mechanism suggests that it should have much broader application. Recall, however, that resting cells in the CA model can become activated even when only one cell connected to it is activated and an activated cell can directly activate every cell to which it is connected. This implies that, for the CA model to be applicable to the more biophysical models, coupling must be strong enough so that spikes are conducted faithfully through gap junctions in the absence of refractoriness. This feature is consistent with the detailed biophysical models of Traub *et al* [26, 28].

Re-entry in the CA model

The network oscillations described in this paper arise from a series of expanding waves initiated by random spontaneous activity. Another mechanism that can generate oscillations in a network of excitable cells is re-entrant behaviour. Re-entry is characterized by persistent activity that circulates around a loop in the network. This circulating activity can drive the entire network at a period set by the time that it takes activity to propagate around the re-entrant loop. In general, the CA model used here does support re-entrant activity; however, re-entry does not occur in our simulations. The explanation below describes how re-entry can start and why it cannot occur in our simulations.

In accordance with the fact that gap junctions often act as symmetric ohmic resistors between cells [13, 14], the connections in the CA model are bidirectional, i.e. activity can flow either way through the connection. This imposes an inherent symmetry on propagated activity arising from point activation. Waves of activity will propagate through all connections present in the network as closed connected surfaces in network connection space. Notice that activity circulating around a loop does not have this symmetry, and therefore the symmetry must be broken in order to obtain re-entrant activity. In the CA model, the only possible way to break the symmetry is for spontaneous activity to occur immediately behind the wave of recovery. This would lead to propagation failure in the direction of the refractory cells and generate a wavefront that is not a closed connected surface. Re-entry will be induced if the shortest cyclic return route to the spontaneously activated cell or 'minimal loop' is longer than the recovery time $t_r + 1$. A similar situation has been described in continuous reaction–diffusion equations [15, 32].

There are two fundamental methods of implementing the effects of spontaneous activity as described in section 4.2. Here and in Traub *et al* [28], all activity is updated simultaneously. In this case, cells immediately behind a wave of recovery cannot be excited and symmetry is always maintained (figure 9(*a*)). If spontaneous activity is not updated simultaneously with propagated activity, the spontaneous activation can occur immediately behind the refractory wave and re-entry can form (figure 9(*b*)).

Oscillations due to re-entry are quite different from those described in this paper. For instance, oscillations due to re-entrant activity are self-sustained (i.e. they do not need input to drive them). The frequency has little or no dependence on the rate of input, but rather is set by the path length of the minimal loop on which the re-entrant activity resides. Furthermore, for networks with connectivity sufficiently above the percolation threshold, the network is composed of very few minimal loops with long path lengths. Because these long loops are scarce, if re-entry is established, it is extremely likely to occur on a short loop. This implies that the frequency of the network oscillations associated with re-entry will be quite high, the peak-to-peak amplitude will be small and the mean level of activity will be high. For a full characterization of re-entrant activity, including frequency and waiting times for induction and annihilation, more work must be done. In particular, the dependence of the distribution of minimal loops on network connectivity must be quantitatively described.

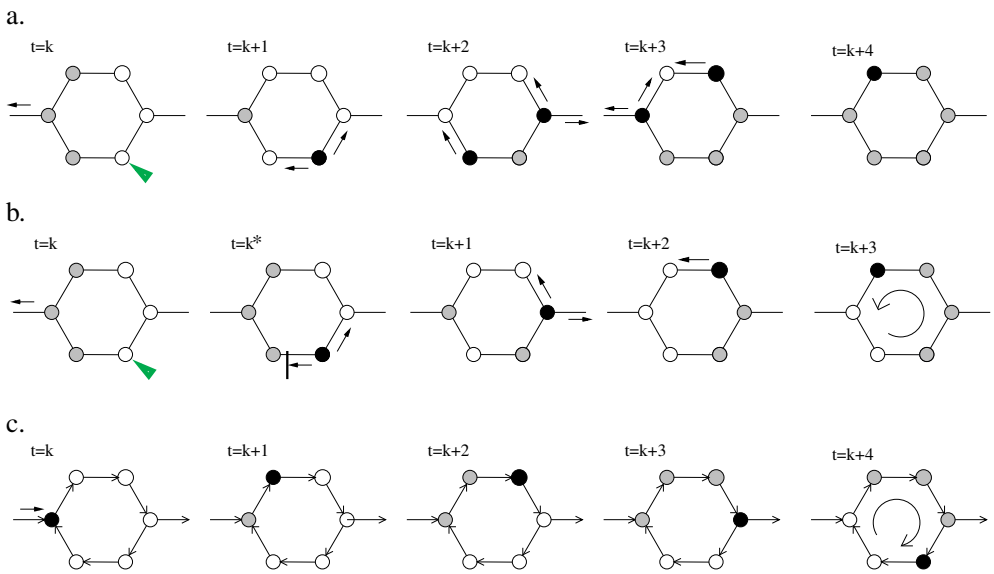

Figure 9. Schematic explanation of how re-entry can or cannot start. Black circles, grey circles, and white circle indicate active cells, refractory cells and resting cells respectively. Thin lines indicate connections between cells and small arrows indicate the spread of activity. Figures (*a*)–(*c*) depict three different scenarios as time (t) progresses. (*a*) A generic minimal loop in a network with bidirectional coupling and simultaneous update of spontaneous events and changes due to coupling rules. At time k, the remains of a leftward-going wave of recovery is seen. A resting cell is selected to spontaneously activate (indicated by thick arrow) and does so at time $k + 1$. Waves of activation then spread in both directions (i.e. symmetrically). The waves collide at the far side of the loop and activity on the loop is annihilated. (*b*) A generic minimal loop in a network with bidirectional coupling and serial update of spontaneous events and then changes due to coupling rules. At time k, the remains of a leftward-going wave of recovery is seen. A resting cell is selected to be spontaneous activated at time k and is activated immediately ($t = k^*$). In this case, activity cannot spread in the direction of the recovery wave. Thus, a wave of activation propagates in only one direction (i.e. symmetry is broken), and re-entrant activity is established. (*c*) A generic minimal loop in a network with unidirectional coupling. Activity spreads to the loop from the left and re-entry is immediately induced.

Networks with chemical synapses

There is one fundamental difference between the unidirectional connectivity of chemical synapses and the bidirectional connectivity of gap junctions that is of special interest here. Activity in a network of neurons connected by gap junctions spreads as closed connected wavefronts; however there is no such symmetry inherent in random networks connected via chemical synapses. Unidirectionally coupled networks are directed graphs and have inherent unidirectional loops (connectivity for some realizations of these networks could turn out to be symmetric, but the probability of observing these realizations is negligible when the networks are sufficiently large). Therefore, in a random network with sparse strong recurrent excitatory synapses, re-entrant activity is almost guaranteed to be induced by a single spontaneous event (see figure 9(*c*)). On the other hand, re-entrant activity can be prevented in a variety of situations, e.g. strong extensive local connectivity so that there are very few minimal loops longer than the refractory period. Note however that although activity in systems without symmetric connectivity can be composed of macroscopic target patterns, there are no true topological target patterns. That is, wavefronts do not always form closed connected surfaces

in network connnection space; a cell apparently outside an expanding wavefront could have a direct connection to cells apparently inside the wavefront. Previous modelling work shows that networks of integrate-and-fire cells exhibit macroscopic target patterns when connections are local and strong [3, 6, 20]. (These target patterns are replaced by re-entrant rhythms when connections are weakened.) The target pattern activity could lead to regular population oscillations in certain parameter ranges and the frequency of these oscillations could be estimated using methods similar to those described in section 5.

Physiological relevance

The detailed biophysical models of Traub *et al* [26, 28] include slow processes such as long-lasting after-hyperpolarizations and slow inhibition. These processes mould activity into bursts of repeated firing separated by periods of no firing. The CA model is constructed only to account for the fast dynamics occurring in the repetitive firing phase. Analysis of the CA model suggests that network oscillations associated with intraburst spiking are due to a series of propagated waves initiated by spontaneous activity. The frequency of the oscillations should have a characteristic dependence on the rate of spontaneous events and on the connectivity footprint of the network. This suggests that the frequency of *in vivo* neural oscillations could be controlled not only by the overall excitatory input rate to a network but also by shunting inhibition located near gap junctions [30], which could control the effective coupling of a network.

The CA model considered here is perhaps the simplest model for networks of randomly connected neurons. In fact, the inability to produce re-entrant behaviour is a result of the symmetry imposed by the simplicity of the CA model. There are several mechanisms by which the symmetry of expanding waves could be broken in many biophysical models of networks of randomly connected neurons. The addition of more complexities to the CA model (to make it 'more realistic') or use of the alternative update scheme can lead to a breakdown of topological target pattern activity and cause re-entrant behaviour to form. Below, we consider a few symmetry breaking mechanisms and suggest situations where they are applicable.

The simultaneous updating scheme that we use in our CA simulations (figure 9(*a*)) does not allow spontaneous activity to induce re-entry, whereas spontaneous activity easily induces re-entry when the alternative update method (figure 9(*b*)) is used. In biophysical models, repetitive spontaneous activity [20] or a single well timed stimulus [15] can cause one-way block, which could lead to re-entry. However, for this to occur, not only must a cell be activated within a precise time window in the recovery period following an action potential [15], but also it must occur along a direct path between gap junctions. In the model of Traub *et al* [28], the spontaneous activity in each cell occurs at a distal portion of the axon, which is not along such a path, and therefore spontaneous activation cannot break symmetry and lead to re-entry. Therefore, the simultaneous updating scheme is perhaps more relevant to the biophysical models of Traub *et al* [26, 28] than the alternative update method.

One modification to the CA that can set up conditions for re-entrant behaviour is the addition of a distribution of refractory periods rather a fixed refractory period. Indeed, it has been shown that re-entry is readily induced in CA models with nearest-neighbour connections when this so-called 'dispersion of refractoriness' is included [19]; this result carries over to our random networks. For re-entrant activity to be induced in a more realistic continuous time model, the heterogeneities in cellular properties must be sufficiently large, whereas introducing a distribution of refractory periods into the CA model immediately imposes a strong heterogeneity because time is coarsely discretized. Thus, one should assess the degree of heterogeneity in the system before adding heterogeneity in the refractory period of cells to the CA model in order to describe dynamics of the actual system more realistically.

More realistic modelling of electrical coupling via gap junctions also introduces processes that could induce re-entry. Coupling in the CA model appears to be consistent with that in networks with strong and sparse connectivity as in the case described by [26, 28], but the CA model fails to capture some of the diffusion characteristics of electrical coupling. For example, in the CA model, an activated cell can directly activate every resting cell to which it is connected, no matter how many. In more realistic systems, when connections are not sufficiently strong or when a cell is connected to many other cells, propagation of activity can fail due to a high diffusive load as a wave propagates through a region in certain directions but not others (effectively due to differences in local branching structures [16]). Analogous behaviour can occur in networks of neurons connected by weak chemical synapses [6, 20]. Thus, the addition of weak connections or graded input to the CA model could lead to re-entry and make our mechanism for oscillations inapplicable. These effects would be magnified by the inclusion of a relative refractory period in the CA model.

In this paper, we used a CA model to identify and characterize a mechanism that could underlie the network oscillations seen experimentally [9, 23] and in the detailed biophysical models of Traub *et al* [26, 28]. Preliminary simulations in a reduced biophysical model of Traub *et al* [28] (a network of only the axonal segments of pyramidal cells connected by axo-axonal gap junctions) with mild heterogeneity in cell properties show that topological target patterns occur over a wide range of parameter space. This supports the applicability of the proposed mechanism, but a focused study of the detailed models and further characterization of activity in the experimental preparations must be done to supply definitive evidence regarding the exact mechanism or combination of mechanisms underlying the network oscillations in these systems.

Acknowledgments

The authors would like to thank Roger Traub for helpful discussions and John Lewis for constructive comments on this manuscript. TJL was supported in part by an NSERC Canada postdoctoral fellowship.

References

[1] Abeles M 1991 *Corticonics: Neural Circuits of the Cerebral Cortex* 1st edn (New York: Cambridge University Press)

[2] Benardo L S 1997 Recruitment of GABAergic inhibition and synchronization of inhibitory interneurons in rat neocortex *J. Neurophysiol.* **77** 3134–44

[3] Beurle R L 1962 Functional organization in random networks *Principles of Self-Organization* ed H von Foerster and G W Zopf (New York: Pergamon) pp 291–314

[4] Butts D A, Feller M B, Shatz C J and Rokhsar D S 1999 Retinal waves are governed by collective network properties *J. Neurosci.* **19** 3580–93

[5] Chow C C and Kopell N 2000 Dynamics of spiking neurons with electrical coupling *Neural Comput.* **12** 1643–78

[6] Chu P H, Milton J G and Cowan J D 1994 Connectivity and the dynamics of integrate-and-fire neural networks *Int. J. Bifurc. Chaos* **4** 237–43

[7] Cobb S R, Buhl E H, Halasy K, Paulsen O and Somogyi P 1995 Synchronization of neuronal activity in hippocampus by individual GABAergic interneurons *Nature* **378** 75–8

[8] Copenhagen D R 1996 Retinal development: on the crest of an exciting wave *Curr. Biol.* **6** 1368–70

[9] Draguhn A, Traub R D, Schmitz D and Jefferys J G R 1998 Electrical coupling underlies high-frequency oscillations in the hippocampus in vitro *Nature* **394** 189–92

[10] Erdös P andÉnyi A R 1960 On the evolution of random graphs *Pub. Math. Inst. Hung. Acad. Sci.* **5** 17–61

[11] Ermentrout G B and Edelstein-Keshet L 1993 Cellular automata approaches to biological modeling *J. Theor. Biol.* **160** 97–133

[12] Feller M B, Butts D A, Aaron H L, Rokhsar D S and Shatz C J 1997 Dynamic processes shape spatiotemporal properties of retinal waves *Neuron* **19** 293–306
[13] Galarreta M and Hestrin S 1999 A network of fast-spiking cells in the neocortex connected by electrical synapses *Nature* **402** 72–5
[14] Gibson J R, Beierlein M and Connors B W 1999 Two networks of electrically coupled inhibitory neurons in neocortex *Nature* **402** 75–9
[15] Glass L and Josephson M E 1995 Resetting and annihilation of re-entrant abnormally rapid heartbeat *Phys. Rev. Lett.* **75** 2059–62
[16] Goldstein S S and Rall W 1974 Changes of action potential shape and velocity for changing core conductor geometry *Biophys. J.* **14** 731–57
[17] Gray C M 1994 Synchronous oscillations in neuronal systems: mechanisms and functions *J. Comput. Neurosci.* **1** 11–38
[18] Greenberg J M and Hastings S P 1978 Spatial patterns for discrete models of diffusion in excitable media *SIAM J. Appl. Math.* **34** 515–23
[19] Kaplan D T, Smith J M, Saxberg E H and Cohen R J 1988 Nonlinear dynamics in cardiac conduction *Math. Biosci.* **90** 19–48
[20] Kistler W M, Seitz R and van Hemmen J L 1998 Modeling collective excitations in cortical tissue *Physica* D **114** 273–95
[21] Llinas R R 1988 The intrinsic electrophysiological properties of mammalian neurons: insights into central nervous system function *Science*
[22] McCormick D A, Wang Z and Huguenard J 1993 Neurotransmitter control of neocortical neuronal activity and excitability *Cereb. Cortex* **3** 387–98
[23] Michelson H B and Wong R K 1994 Synchronization of inhibitory neurones in the guinea-pig hippocampus in vitro *J. Physiol. (Lond)* **92** 35–45
[24] Stauffer D and Aharony A 1992 *Introduction to Percolation Theory* (Washington, DC: Taylor and Francis)
[25] Steriade M 1997 Synchronized activities of coupled oscillators in the cerebral cortex and thalamus. *Cereb. Cortex* **7** 583–604
[26] Traub R D 1995 Model of synchronized population bursts in electrically coupled interneurons containing active dendrites *J. Comput. Neurosci.* **2** 283–9
[27] Traub R D, Jefferys J G and Whittington M A 1999 *Fast Oscillations in Cortical Circuits* 1st edn (Cambridge, MA: MIT Press)
[28] Traub R D, Schmitz D, Jefferys J G and Draguhn A 1999 High-frequency population oscillations are predicted to occur in hippocampal pyramidal neural networks interconnected by axo-axonal gap junctions *Neuroscience* **92** 407–26
[29] Tyson J J and Keener J P 1988 Singular perturbation theory of traveling waves in excitable media *Physica* D **32** 327–61
[30] Welsh J P, Lang E J, Sugihara I and Llinas R 1995 Dynamic organization of motor control within the olivocerebellar system *Nature* **374** 453–7
[31] Wiener N and Rosenblueth A 1946 The mathematical formulation of the problem of conduction of impulses in a network of connected excitable elements, specifically in cardiac muscle *Arch. Inst. Cardiol. Mex.* **16** 205–65
[32] Winfree A T 1983 Sudden cardiac death, a problem in topology *Sci. Am.* **248** 114–61